Iranian Journal of Chemical Engineering, 17 (2), 56-69, (2020) pISSN: 1735-5397
DOI: 10.22034/ijche.2020.253425.1354 eISSN: 2008-2355

Developing a Mathematical Correlation to Predict the Behavior of a Supersonic Superheated Steam Flow Inside a Laval Nozzle

***H. Rezaei*[1], *S. Ovaysi*[2*], *M. Rahimi*[2]**

[1] *Department of Chemical Engineering, Kermanshah Branch, Islamic Azad University, Kermanshah, Iran*
[2] *Faculty of Petroleum and Chemical Engineering, Razi University, Kermanshah, Iran*

ARTICLE INFO

Article history:
Received: 2020-10-19
Accepted: 2020-11-04

Keywords:
Laval Nozzle,
Mathematical Correlation,
Mach Number,
Decision Parameters,
Supersonic Flow,
Superheated Steam

ABSTRACT

The objective of the investigation was to mathematically correlate the behavior of a supersonic superheated steam flow inside a Laval nozzle, with the decision parameters. The decision parameters are the inlet temperature ranging from 374.3 K to 504.3 K and the inlet pressure ranging from 40050.14 Pa to 133375.7 Pa. Indeed, the outlet temperature, outlet pressure as well as the Mach number mathematically correlate with the decision parameters. The numerical approach based on the Computational Fluid Dynamics (CFD) is selected to study the behavior of the supersonic superheated steam flow inside the nozzle. By examining the different temperature and pressure conditions of the inlet fluid, it was found that the closest distance from the starting point of condensation to the throat was at the highest pressure and lowest temperature. Conversely, the farthest distance from the starting point of condensation to the throat is at the lowest pressure and highest temperature. In addition, three mathematical correlations were developed. Due to the high accuracy of the mathematical correlations, the efficiency of the predictor models in predicting the outputs was proved.

1. Introduction

In the supersonic flows, some of the common phenomena are the drop formation and its growth. It happens in a wide verity of natural processes and industries such as the steam flow in turbines, supersonic separations and all convergent-divergent nozzles. Therefore, the recognition and understanding of the phase change in this process are of significant importance, when the phase transition occurs under the high super saturation achieved in the rapid expansions [1, 2].

The study of condensation in Converging-diverging nozzles has always been important significantly. In these nozzles, since the cross-section area decreases until reaching the throat area (in which the Mach number reaches unity), the flow velocity increases along with the nozzle which in turn leads to an increase in the velocity in this equipment and consequently the static enthalpy decreases. In addition, by passing through the throat area, the Mach number exceeds unity, and by considering the increasing cross-section area, the flow velocity increases. Hence, increasing the flow velocity results in a decrease in the temperature and pressure along the Laval nozzle [3-6].

Yang et al. [7] modified the Internal Consistent Classical Nucleation Theory

[*]Corresponding author: s.ovaysi@razi.ac.ir, s.ovaysi@gmail.com

(ICCT) to predict the condensing phenomenon inside a two-dimensional Laval nozzle. Gyarmathy's approach was employed to model the droplet growth and also develop the two-phase Euler-Euler flow model.

The Internal Consistent Classical Nucleation Theory (ICCT) was improved by Bian et al. [1]. In the research, a high-pressure condensable flow in the Laval nozzle was studied using a mathematical model, based on the ICCT approach. Yang et al. [2] developed a compressible numerical model in a conventional Laval nozzle. In the investigation, the Eulerian-Eulerian approach was employed to predict the non-equilibrium condensing phenomenon. The applied method was shown as an efficient technique to predict pressure distributions, droplet sizes and mixture conditions for inviscid flows.

Halama et al. [8] presented three Eulerian models, 0-equation, 2-equation, and 4-equation, to predict the non-equilibrium condensation phenomenon in a convergent-divergent nozzle. It was demonstrated that the 0-equation model was suitable to approximate a non-equilibrium condensable steam flow. In another study, the CEOS/GE models were employed to predict the vapor-liquid equilibrium [9]. Gerber et al. [10] considered the spontaneous homogeneous nucleation for the nucleated steam. A two-phase Eulerian-Lagrangian model was employed to investigate the interaction between vapor and droplet phases, gas and liquid phases, in the Laval nozzle flows. Since the two phases do not have to share the same velocity field, the Eulerian-Lagrangian approach has the potential for combining much more complex droplet behaviors.

Ding et al. [11] evaluated the effect of different parameters, with a wide verity of swirl strengths, inside the supersonic separator and also studied the dehydration performances of a separator. The supersonic separator was utilized to purify the natural gas at high pressures and low temperatures [12-14]. The nucleation rate, droplet numbers, droplet radius and droplet fraction, were analyzed in the study.

Niknam et al. [15, 16] analyzed the supersonic separation for predicting the relevant performance and presented an efficient model for the 3S using MATLAB, COMSOL and HYSYS softwares. Liu et al. [17] discussed a three-dimensional geometry of a convergent-divergent nozzle. The Reynolds Stress Model (RSM) was applied during the simulation process. The homogenous equilibrium model (HEM) was used by Asadollahi [18] to calculate the pressure drop of a two-phase flow. Heidari et al. [19] discussed the dynamic behavioral differences among various nucleation and growth models. Based on the obtained results, a clearly recognizable relation is observed between the pressure and shockwave location inside the nozzle. Thus, reducing the downstream resistance of the nozzle is an effective way to enhance the performance of the supersonic separator.

A large number of experiments were performed to study the nucleation phenomenon in different pressure and temperature conditions in Laval nozzles by Moses et al. [29]. Since there is no clearly simple relationship between the properties of water vapor such as enthalpy and temperature and pressure, the accurate analysis of the steam flow is not an easy issue in Laval nozzles. Moreover, due to the expansion of water vapor into the saturation region in the nozzles, the analysis becomes more complicated.

The current study attempts to generalize a

mathematical correlation between a wide variety of the decision parameters to describe and model the behavior of the supersonic superheated steam flow inside a Laval nozzle.

The effect of the inlet temperature and pressure of the nozzle on the condensation as well as the Mach number for a converging-diverging nozzle is considered. Three different mathematical correlations are developed to calculate the outlet temperature, outlet pressure as well as the Mach number.

Table 1
A summary of previous researches on the condensation process and supersonic flows.

Authors	Geometry	Method	Phase	Purpose
Yang et al. [20]	Supersonic steam ejectors	CFD (Fluent)	Wet steam	Evaluating the performance of steam ejectors
Zhang et al. [21]	Steam turbine	CFD (Fluent)	Wet steam	Optimizing the dehumidification effect and wetness loss
Kuan et al. [22]	Laval nozzle	CFD (CFX)	Mg vapor	Investigating the effect of heat and mass transfers on the CNT model
Teixeira et al. [23]	Supersonic separator	ASPEN HYSYS	Natural gas	Removing condensable vapors from the gas flow
Wang and Hu [24]	Supersonic separator	Experimental and numerical	Natural gas	Investigating the effect of swirling generator and drainage structure
MA et al. [25]	Laval nozzle	CFD	Water vapor	Calculations of nucleating moist gas and wet steam
Bian et al. [26]	Supersonic separator	CFD (Fluent)	Methane vapor	Investigating the effect of swirling on the condensation process
Ding et al. [27]	Sonic nozzle	CFD	Moist air	Studying the condensation process of water vapor at the moist air
Ding et al. [28]	Nozzle	CFD	Pure steam	Presenting the Wilson Point-related equations

2. Numerical study

The governing equations are solved using the Computational Fluid Dynamics (CFD) technique via the ANSYS FLUENT R2 2019. A 3D simulation was made in this study. The Eulerian-Eulerian approach was utilized for modelling the condensation phenomenon. The governing equations are included in the simulation [7]. Two other transfer equations are also considered to simulate the condensation phenomenon [30, 31]. The inlet and outlet pressures were selected as the boundary conditions of the Laval nozzle. The transient state solution is used, and the time step is adjusted at 10-6. Absolute criteria of convergence were set at 10-4, 10-3 and 10-6 for energy, continuity and other variablesrespectively. The second-order upwind discrete scheme was selected for the spatial discretization. A survey was conducted among the turbulence models, RNG K-epsilon, SST (Shear Stress Turbulence), K-omega and RSM (Reynolds Stress Model). The K-ω model was selected as the proper turbulence model because it had the least error among turbulence models.

3. Results and discussion

In the investigation, an accurate mathematical correlation, between the decision parameters, was generalized to model the behavior of the supersonic superheated steam flow inside a Laval nozzle. A wide range of the tests is undertaken at low pressures and high temperatures by Moses et al. [29]. In that research, a wider range of the pressures and temperatures is considered as compared with the work of Moses. It is worth mentioning that, Moses et al. [29] used that range to study the nucleation models and droplet growth while, that range was employed to investigate the behavior of the pressure, temperature as well as the Mach Number along the Laval nozzle and also to correlate them by three accurate equations at the outlet of the nozzle in the study.

The decision parameters were the inlet temperature in 14 levels ranging from 374.3 K to 504.3 K and the inlet pressure in 15 levels of 40050.4 Pa to 133375.7 Pa. Indeed, the outlet temperature, outlet pressure as well as the Mach number are mathematically correlated to the decision parameters. The numerical approach based on the Computational Fluid Dynamics (CFD) was employed to study the behavior of the supersonic superheated steam flow inside the nozzle.

3.1. Grid independency check

The simulated nozzle has been designed based on the size of the Laval nozzle in the Moses's experimental model. Figure 1, presents the 3D and 2D schemes of the simulated Laval nozzle in this paper. The grid independence test was undertaken to ensure the numerically obtained results. The inlet pressure and temperature were set at 66807.84 Pa and 385.15 K respectively. Figure 2 describes the differences among a various number of meshes in modeling the Mach number along the Laval nozzle. The Mach number attains the value of 1 at x=8.22 cm with a cross section area of 1 cm^2. As an overall trend, the Mach number always increases for all cases except around X=11.2 cm, where an oscillation is observed, which indicates the differences among the numbers of meshes (n). Thus, there is a clearly recognizable relationship between the grid density and the results of the simulation. Therefore, the differences among the gride densities of n=23952, n=57664, and n=220659 are evident. Indeed, the errores are negligible for n=911692 and n=3737067. Thus, n=911692 is recognized as the optimal number of meshes.

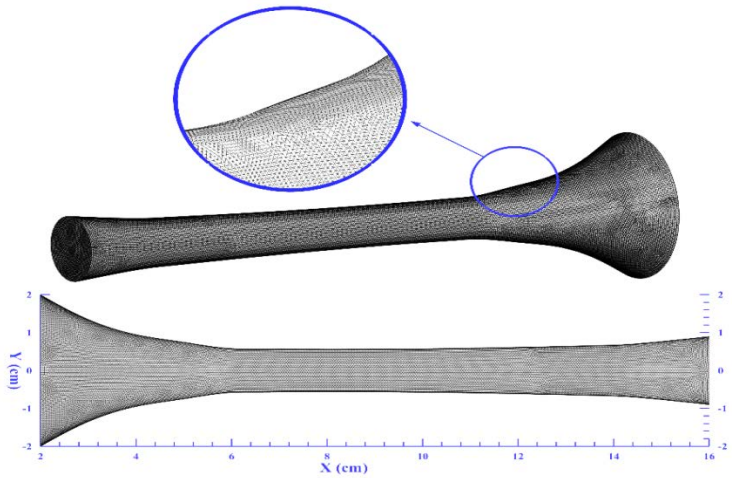

Figure 1. The geometry of the studied Laval nozzle.

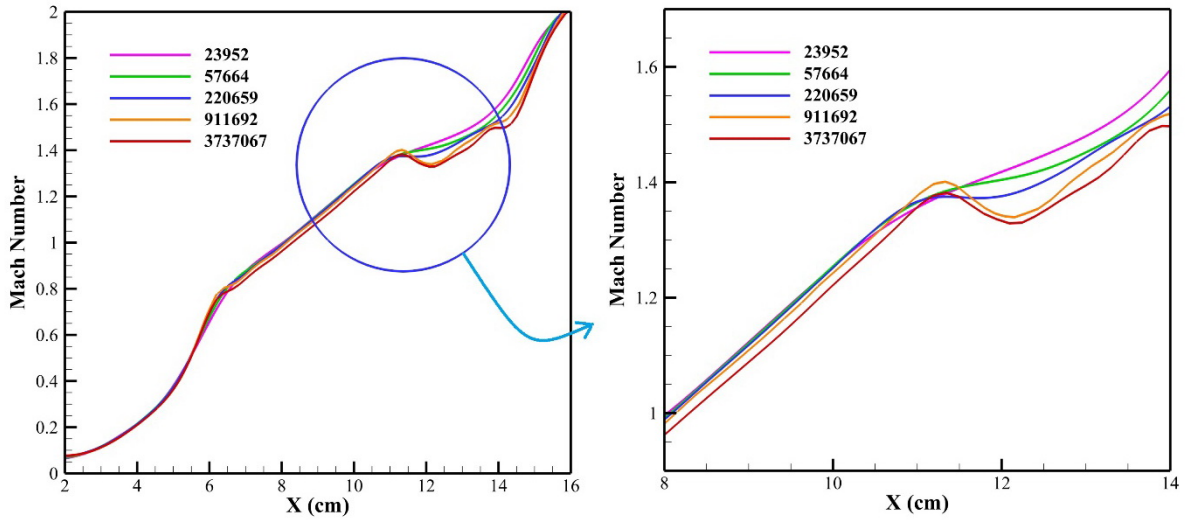

Figure 2. The effect of the mesh number (*n*) on the numerical results.

3.2. Model validation

Among Moses's experiments [29], test No. 421, in which the inlet pressure and temperature are 66807.84 Pa and 385.15 K respectively, is selected for the validation study. Thus, the non-dimensional experimentally obtained pressure values are used to validate the numerically obtained ones. As shown in Figure 3, it is proved that the numerical model is of a high potential to predict the behavior of the flow inside the Laval Nozzle. As the figure shows, with change in distance along the nozzle, the X axis(cm), the non-dimensional pressureand the Y axis values gradually decreases, ranging from X=11.5 cm to X=12 cm. Beyond this range, again, it starts to increase moderately, which is caused by the latent heat exchang through thevapor to liquid transtion. Since the nucleation phenomenon happens at a part of its length, just a portion of nozzle length ranging from 8 to 14 cm is shown in Figure 3.

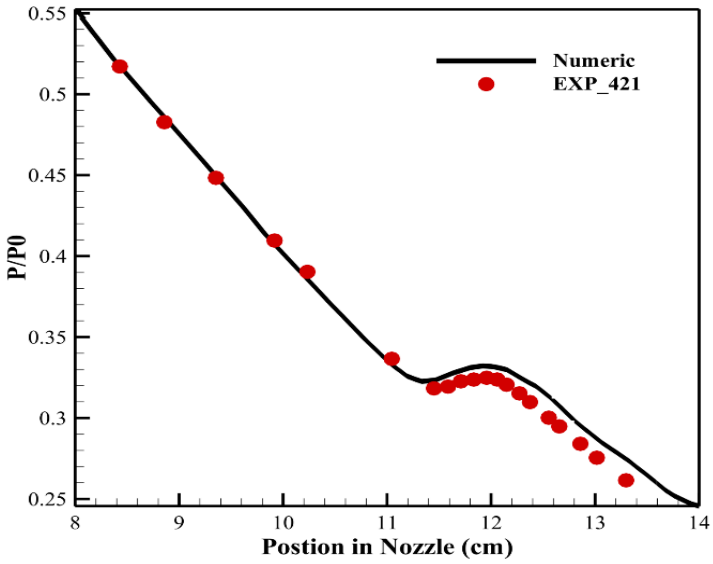

Figure 3. Numerical results as compared to the experimental ones by Moses [29].

Figures 4 and 5 depict the trend of the pressure and temperature along the Laval nozzle respectively. As an overall trend, the pressure and the temperature decrease due to

the increase in the velocity along the Laval nozzle. As shown in the figures, an upward trend in a short length is observed in the behavior of both temperature and pressure at the same length and position, in the range of X=11.5 cm to X=12 cm. It can be deduced that the latent heat variation in the condensation process increases the temperature and, finally, heats the vapor phase. The temperature and pressure at the inlet of the Laval nozzle have been set as 70660.85 Pa and 377.15 K respectively.

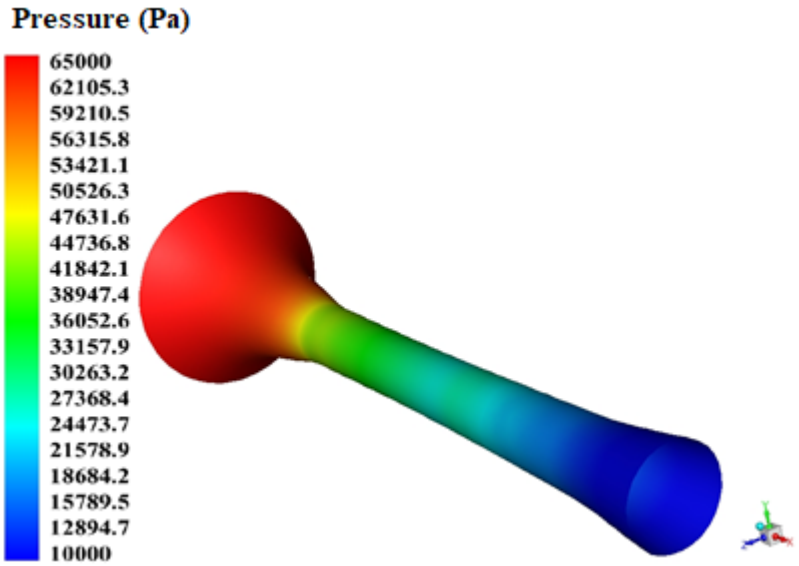

Figure 4. Numerically obtained pressure (Pa) along the Laval nozzle.

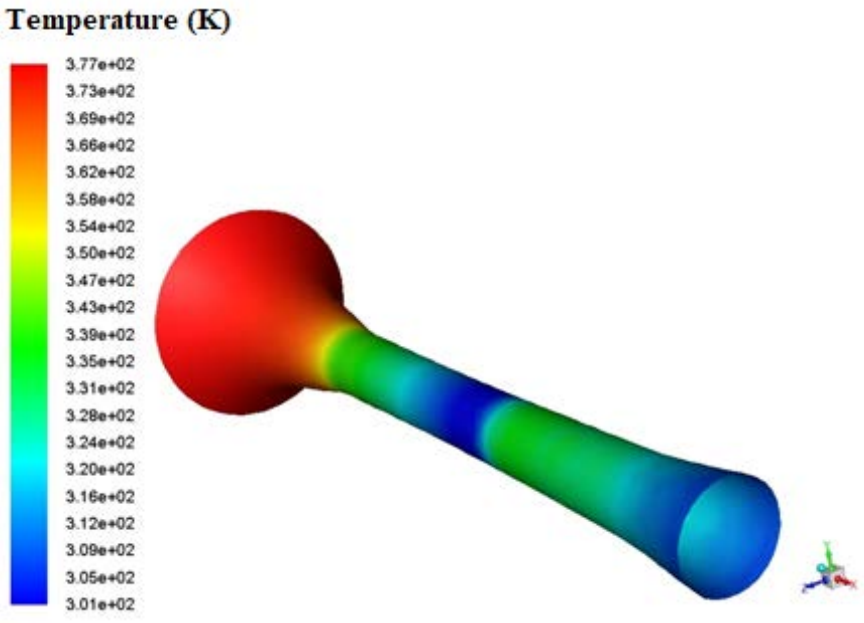

Figure 5. Numerically obtained temperature (K) along the Laval nozzle.

Figures 6 and 7 provide the variations of the pressure and Mach number along the nozzle at five different input temperatures ranging from 474.15 K to 504.15 K. These variations have been represented at four different input pressures ranging from 40050.14 Pa to 133375.7 Pa.

As shown in Figure 6, decrease in the

nozzle inlet temperature leads to the position of expansion approaching the throat. On the other hand, at various constant input temperatures, increasing the input pressure lets the position of expansion be closer to the throat. Generally, the shortest distance between the throat and the starting point of expansion corresponds to the lowest temperature and the highest pressure. This can be explained that increasing the inlet temperature of the nozzle will result in decreasing the degree of the supercooling of vapor, under the same inlet pressure. Thereby, it's relatively harder to reach the critical conditions for nucleation.

Figure 7 shows the changes in the Mach number under different temperature and pressure conditions. The increasing trend of the Mach number at different temperatures is quite clear. A decrease of the Mach number is seen along the nozzle showing that the starting point is different for various input conditions. The starting point for decreasing the Mach number for each temperature is equal to the starting point for increasing the pressure for each temperature in the Fig. 6. Finally, as the temperature increases, the starting point of condensation moves away from the throat, while with increasing the pressure, the point of condensation approaches the throat. As in Figure 6, the nearest condensation point is at a low temperature and high pressure, and the farthest condensation point is at a low pressure and high temperature.

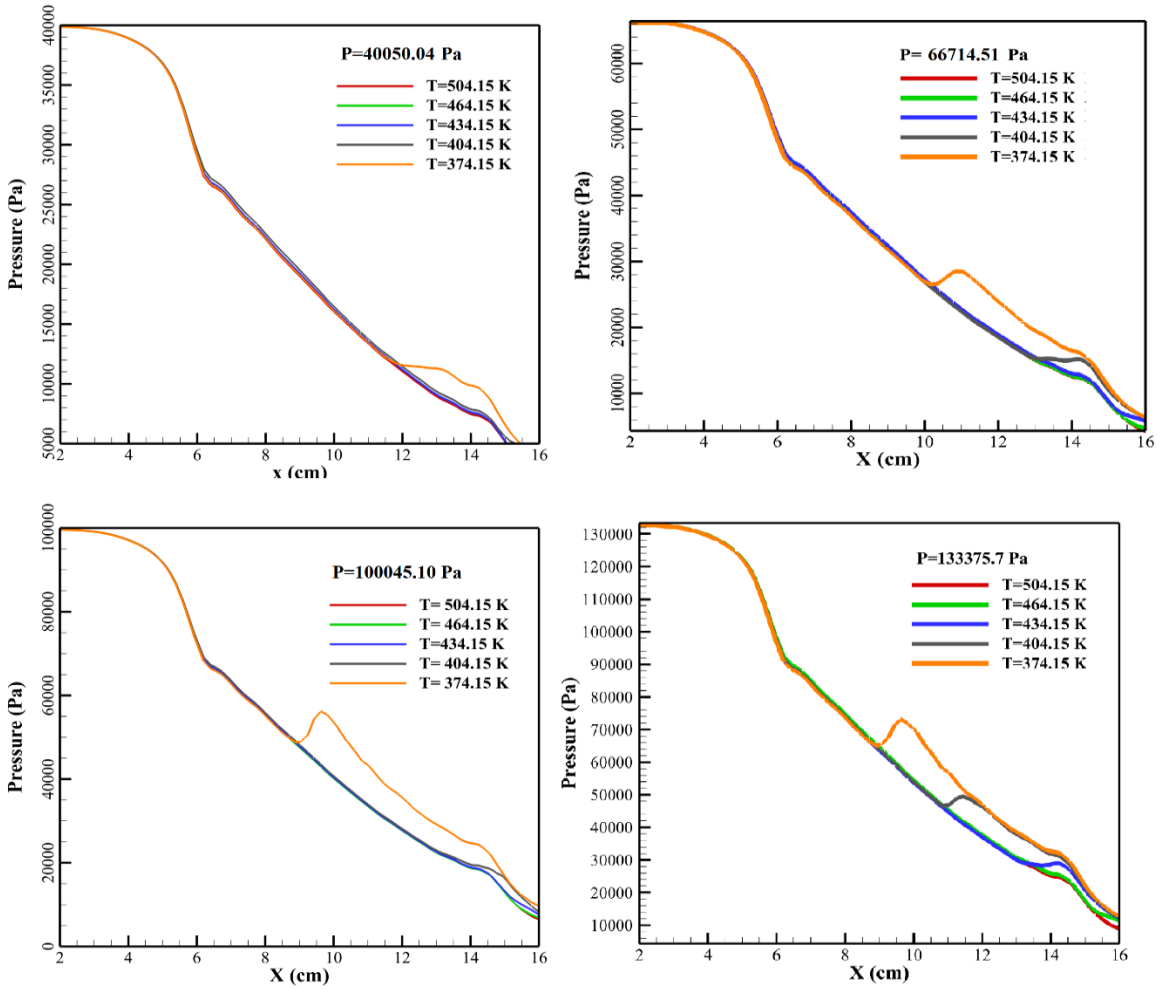

Figure 6. The variation of the pressure along the nozzle in different temperatures.

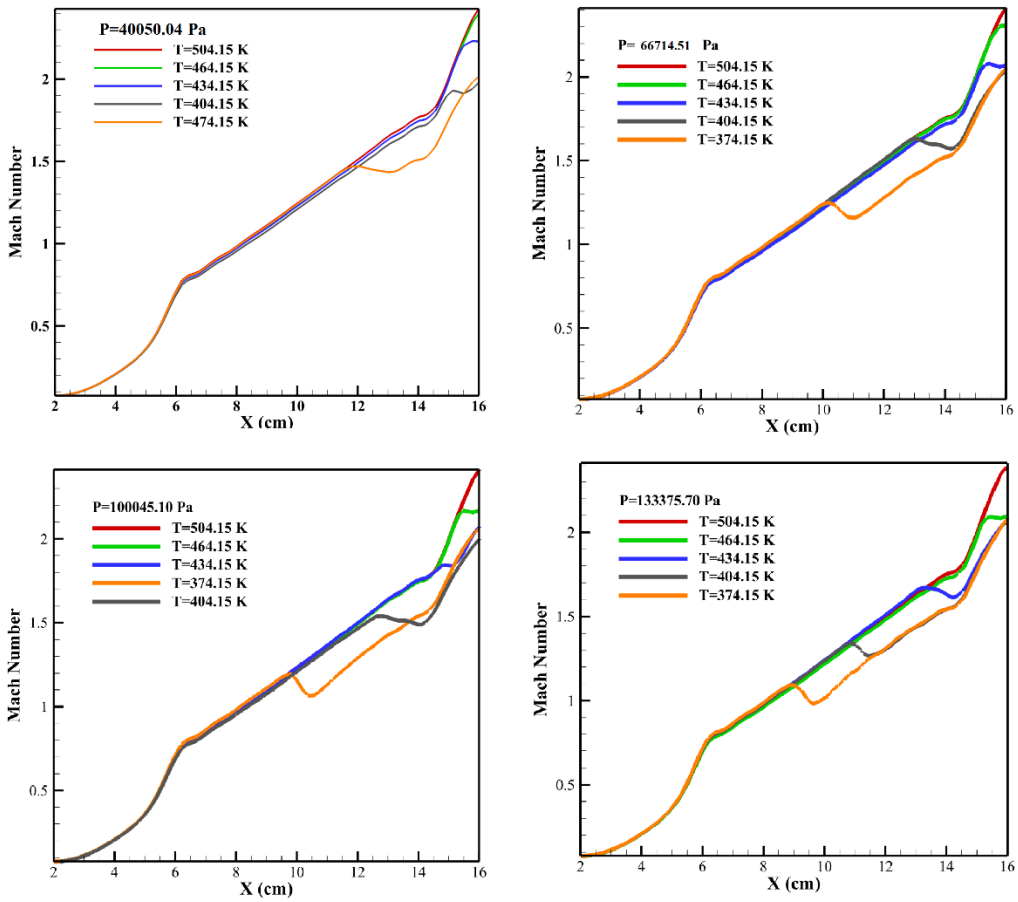

Figure 7. The variation of the Mach number along the nozzle in different temperatures.

In the next step, the outlet temperature (T_{out}), outlet pressure (P_{out}) as well as the Mach number (Ma) as the numerically obtained outputs are predicted by a correlation with the least error. According to this, three correlations are generalized to express the relation between the output parameters including the outlet temperature (T_{out}), outlet pressure (P_{out}) as well as the Mach number (Ma), and the input (design) parameters including the inlet temperature (T_{in}) and the inlet pressure (P_{in}) with a good accuracy as follows:

$$T_{out} = 262 + 18.45T_{in} + 12.72\exp(-P_{in}/70) - 0.487T_{in}^2 + 8.382T_{in}\exp(-P_{in}/70) \quad (1)$$

$$P_{out} = 6.9567\times10^6 + 2.7597\times10^6 T_{in} + 0.9960\times10^6\exp(-P_{in}/70) + 0.0188\times10^6 T_{in}^2 + 0.5687\times10^6 T_{in}\exp(-P_{in}/70) \quad (2)$$

$$Ma = 2.363 - 0.006912T_{in} - 0.003816\exp(-P_{in}/35) \quad (3)$$

In fact, the above correlations in relevant forms have been recognized by the MATLAB 2019b software to achieve the best-predicted results. For this purpose, a number of popular functions in mathematics have been tested and eventually one of them was selected for developing the mathematical correlation. Indeed, the correlations in the aforementioned forms are picked up as the best mathematical correlations which precisely describe the behavior of the outlet temperature (T_{out}), outlet pressure (P_{out}) as well as the Mach

number (Ma) in terms of the design parameters. Figure 8 shows the outlet temperature (T_{out}), the outlet pressure (P_{out}) as well as the Mach number (Ma) predicted by the proposed correlation, along all numerically obtained ones.

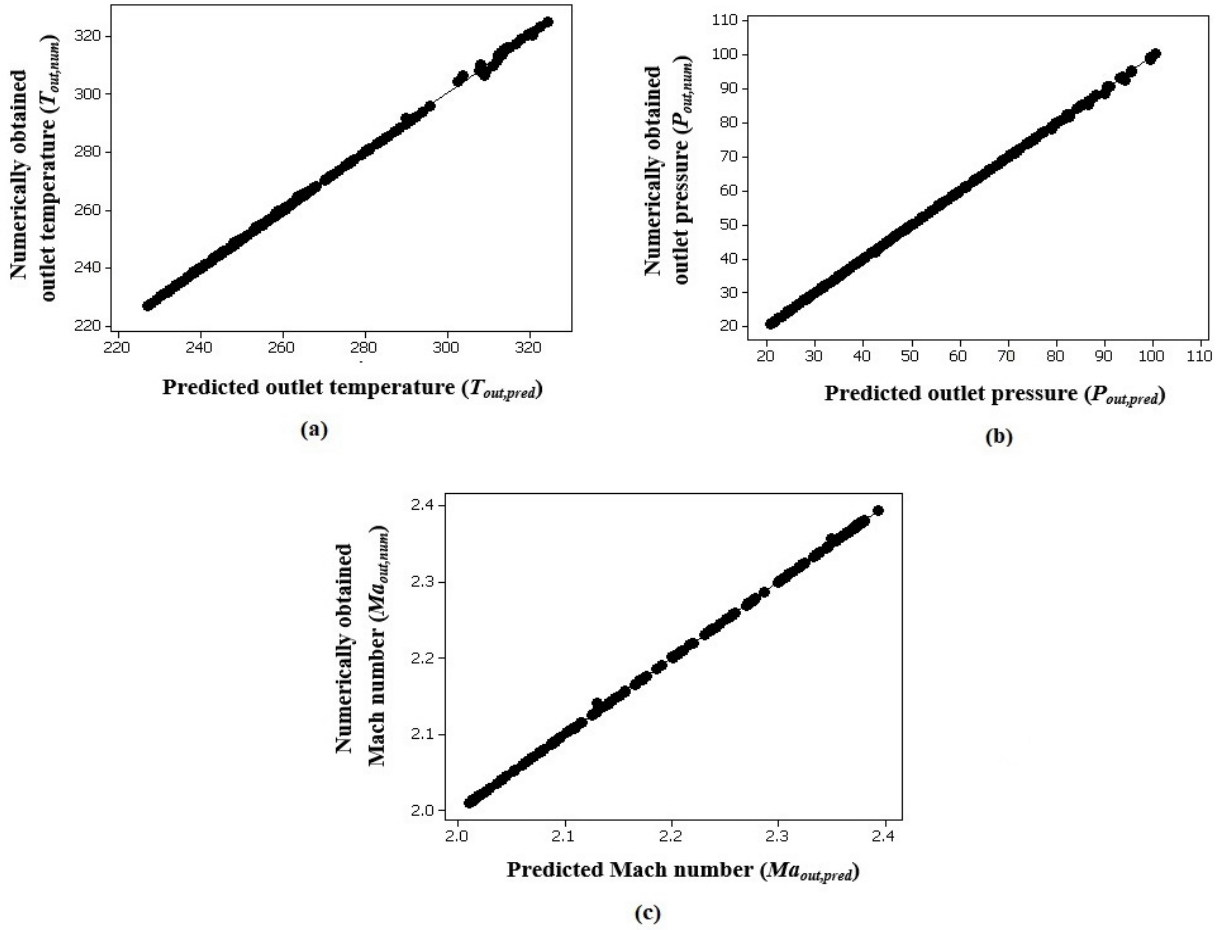

Figure 8. Numerically obtained: a) outlet temperature (T_{out}), b) outlet pressure (P_{out}), c) Mach number (Ma), against the predicted ones by the empirical correlation.

The forecast performance of the suggested correlation is evaluated through the sum-squared errors (SSE), coefficient of determination (R^2), coefficient of partial determination (Adjusted R^2), mean relative error (MRE), root-mean square error (RMSE), and standard deviation (STD) values, which are calculated as follows:

$$SSE = \sum_{i=1}^{N} (O_{Num,i} - O_{Pred,i})^2 \quad (4)$$

$$R^2 = 1 - \frac{SSE}{\sum_{i=1}^{N} O_{Num,i}^2} \quad (5)$$

$$\text{Adjusted } R^2 = 1 - \left(\frac{(1 - R^2) \times (DFE - 1)}{DFE - m - 1} \right) \quad (6)$$

$$MRE\ \% = \frac{1}{N} \sum_{i=1}^{N} \left| \frac{O_{Num,i} - O_{Pred,i}}{O_{Num,i}} \right| \times 100 \quad (7)$$

$$RMSE = \sqrt{\frac{SSE}{DFE}} \quad (8)$$

$$STD = \sqrt{\frac{SSE}{DFE - 1}} \quad (9)$$

where, N indicates the number of data, m is the number of decision parameters, DFE represents the degree of freedom, and $O_{Num,i}$

and $O_{Pred,i}$ refer to numerically obtained and predicted values respectively.

The error information of the proposed mathematical correlations, in predicting the outlet temperature (T_{out}), the outlet pressure (P_{out}), as well as the Mach number (Ma), has been presented in Table 2. From this Table, the MRE % and SSE for predicting the outlet temperature (T_{out}) have been found to be 0.1042 % and 5.169 respectively. In addition, the proposed statistical features for the outlet pressure (P_{out}) is 0.1170 % and 0.7343 respectively. Moreover, for the Mach number (Ma), the aforementioned features are 0.0045 % and 4.242×10^{-5} respectively. Based on the results indicated in Fig. 8 and Table 2, it is proved that the aforementioned correlations are characterized as good predictor models in the investigation.

Table 2
The accuracy of the proposed correlations in comparison with the numerically obtained results, for the average outlet temperature (T_{out}), outlet pressure (P_{out}) as well as the Mach number (Ma).

No.	Output	MRE %	Number of coefficients	DFE	SSE	R^2	R^2 (Adjusted)	RMSE	STD
1	Outlet temperature (T_{out})	0.1042	5	205	5.169	0.986	0.9857	0.1588	0.1681
2	Outlet pressure (P_{out})	0.1170	5	205	0.7343	0.9969	0.9968	0.0598	0.0171
3	Mach number (Ma)	0.0045	3	207	4.242×10^{-5}	0.9595	0.9591	0.0004	0.0014

As the last step, through the statistical analysis, it is determined that how much of the outlet temperature (T_{out}), the outlet pressure (P_{out}) as well as the Mach number (Ma) are affected by each of the decision parameters. As a matter of fact, the quantitative effect of each decision parameter, including the inlet temperature (T_{in}) and the inlet pressure (P_{in}) on the aforementioned measured outputs are separately specified. Figure 9 presents the quantitative effects of the decision parameters on the measured outputs. As the statistical results in Figure 9 indicate, the inlet pressure (P_{in}) has more influence on the outlet temperature (T_{out}) than on the inlet temperature (T_{in}). In addition, similarly, the inlet pressure (P_{in}) has more influence on the outlet pressure (P_{out}) than on the inlet temperature (T_{in}). In contrast, the inlet pressure (P_{in}) has more influence on the Mach number (Ma) than on the inlet temperature (T_{in}). What is understood from the following figures is that, the outlet temperature (T_{out}), the outlet pressure (P_{out}) as well as the Mach number (Ma) can quantitatively be controlled by the proper setting of the inlet temperature (T_{in}) and inlet pressure (P_{in}). Indeed, the greater the portion of each design parameter is, the larger the effect of that parameter can be seen. Consequently, it has a greater role in controlling the relevant output parameter.

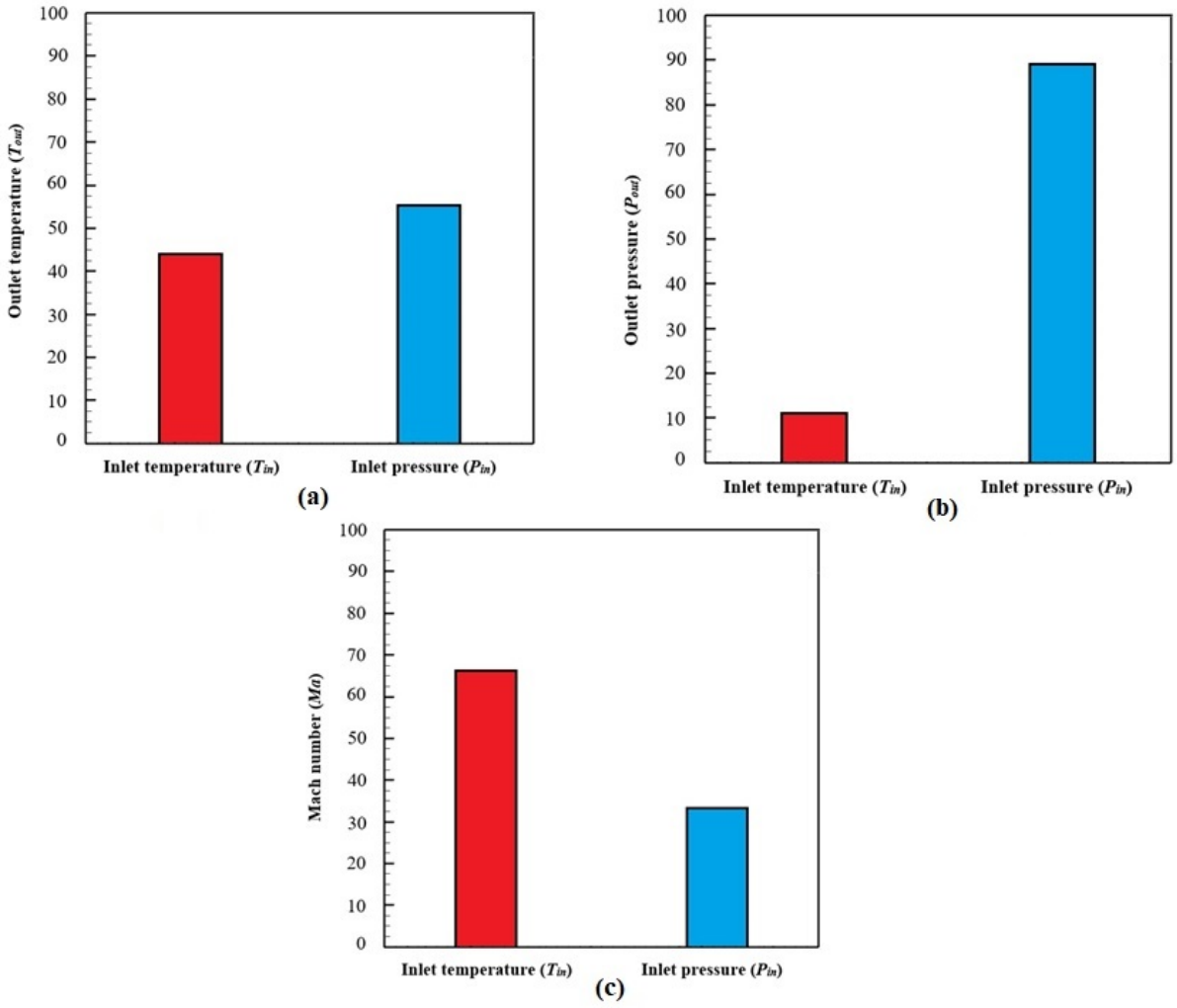

Figure 9. The quantitative effect of the decision parameters on the a) outlet temperature (T_{out}) b) outlet pressure (P_{out}) c) Mach number (Ma).

4. Conclusions

Laval nozzles have widely been utilized to investigate the condensation of condensable gases and pure vapors, particularly steam. The main objective of the current study is to generalize a mathematical correlation, between the decision parameters, to model the behavior of the supersonic superheated steam flow inside a Laval nozzle. The decision parameters are the inlet temperature (T_{in}) in 14 levels ranging from 374.3 K to 504.3 K and the inlet pressure (P_{in}) in 15 levels from 300.4 Pa to 1000.4 Pa. Indeed, the outlet temperature, the outlet pressure as well as the Mach number are mathematically correlated with the decision parameters. The CFD modeling was carried out for this purpose. It was found that, the inlet pressure (P_{in}) has more influence on the outlet temperature (T_{out}) than on the inlet temperature (T_{in}), with around 10 % difference. In addition, similarly, the inlet pressure (P_{in}) has more influence on the outlet pressure (P_{out}) than on the inlet temperature (T_{in}), with around 80 % difference. In contrast, the inlet pressure (P_{in}) has more influence on the Mach number (Ma) than on the inlet temperature (T_{in}), with around 35 % difference. Also, the outlet temperature (T_{out}), the outlet pressure (P_{out}) as well as the Mach number (Ma) can

quantitatively be controlled by the proper setting of the inlet temperature (T_{in}) and inlet pressure (P_{in}). Furthermore, three mathematical correlations, between the decision parameters with least error values, are developed for the outlet temperature, the outlet pressure, as well as the Mach number.

Nomenclature

m	number of decision parameters.
Ma	Mach number.
N	number of data.
P	pressure [Pa].
P_{in}	inlet pressure.
P_{out}	outlet pressure.
R^2	coefficient of determination.
T	temperature [K].
T_{in}	inlet temperature.
T_{out}	outlet temperature.
Adjusted R^2	coefficient of partial determination.
CEOS	cubic equation of state.
CFD	computational fluid dynamics.
DFE	degree of freedom.
GE	excess molar Gibbs energy.
MRE	mean relative error.
RMSE	root-mean square error.
STD	standard deviation.
SSE	sum-squared errors.

References

[1] Bian, J., Cao, X., Yang, W., Guo, D. and Xiang, Ch., "Prediction of supersonic condensation process of methane gas considering real gas effects", *Applied Thermal Engineering*, **164**, 114508 (2020).

[2] Yang, Y. and Shen, Sh., "Numerical simulation on non-equilibrium spontaneous condensation in supersonic steam flow", *International Communications in Heat and Mass Transfer*, **36**, 902 (2009).

[3] Wyslouzil, B. E., Wilemski, G., Beals, M. G. and Frish, M. B., "Effect of carrier gas pressure on condensation in a supersonic nozzle", *Physical Sciences Inc.*, **6** (8), 2845 (1998).

[4] Gerber, A. G. and Kermani, M. J., "A pressure based Eulerian-Eulerian multi-phase model for non-equilibrium condensation in transonic steam flow", *International Journal of Heat and Mass Transfer*, **47**, 2217 (2004).

[5] Simpson, D. A. and White, A. J., "Viscous and unsteady flow calculations of condensing steam in nozzles", *International Journal of Heat and Fluid Flow*, **26**, 71 (2005).

[6] Cengel, Y. A. and Boles, M. A., Thermodynamics an Engineering Approach, 3rd Ed., McGraw-Hill Higher Education, Michigan, p. 869 (2006).

[7] Yang, Y., Walther, J. H., Yan, Y. and Wen, Ch., "CFD modeling of condensation process of water vapor in supersonic flows", *Applied Thermal Engineering*, **115**, 1357 (2017).

[8] Halama, J. and Hric, V., "Numerical solution of steam flow in a nozzle using different non equilibrium condensation models", *Applied Mathematics and Computation*, **115**, 1 (2015).

[9] Basirat, M. and Fathikalajahi, J., "Prediction of vapor-liquid equilibria using CEOS/GE models", *International Journal of Chemical Engineering*, **2** (1), 71 (2005).

[10] Gerber, A. G., "Two-phase Eulerian/Lagrangian model for nucleating steam flow", *Journal of Fluids Engineering*, **124**, 465 (2002).

[11] Ding, H., Sun, Ch., Wang, Ch., Wen, Ch. and Tian, Y., "Prediction of dehydration performance of supersonic separator

based on a multi-fluid model with heterogeneous condensation", *Applied Thermal Engineering*, 171, 115074 (2020).

[12] Cao, X. W. and Yang, W., "Numerical simulation of binary-gas condensation characteristics in supersonic nozzles", *Journal of Natural Gas Science and Engineering*, **25**, 197 (2015).

[13] Malyshkina, M. M., "The procedure for investigation of the efficiency of purification of natural gases in a supersonic separator", *High Temperature*, **48**, 244 (2010).

[14] Wen, Ch., Cao, X., Yang, Y. and Zhang, J., "Swirling effects on the performance of supersonic separators for natural gas separation", *Chem. Eng. Technol.*, **34**, 1575 (2011).

[15] Niknam, P. H., Mortaheb, H. R. and Mokhtarani, B., "Optimization of dehydration process to improve stability and efficiency of supersonic separation", *Journal of Natural Gas Science and Engineering*, **43**, 90 (2017).

[16] Niknam, P. H., Mortaheb, H. R. and Mokhtarani, B., "Effects of fluid type and pressure order on performance of convergent-divergent nozzles: An efficiency model for supersonic separation", *Asia, Pac. J. Chem. Eng.*, **13**, 2181 (2018).

[17] Liu, X. and Liu, Zh., "Numerical investigation and improvement strategy of flow characteristics inside supersonic separator", *Separation Science and Technology*, **53**, 940 (2017).

[18] Asadollahi, M., "Two-phase flow pressure drop calculation using homogeneous equilibrium model", *Iranian Journal of Chemical Engineering (IJChE)*, **16** (3), 84 (2019).

[19] Heidari, A. and Shirvani, M., "Effect of different nucleation and growth kinetic terms on modeling results of KNO_3 CMSMPR crystallizer", *Iranian Journal of Chemical Engineering (IJChE)*, **10** (1), 79 (2013).

[20] Yang, Y., Zhu, X., Yan, Y., Ding, H. and Wen, Ch., "Performance of supersonic steam ejectors considering the nonequilibrium condensation phenomenon for efficient energy utilisation", *Applied Energy*, **242**, 157 (2019).

[21] Zhang, G., Wang, F., Wang, D., Wu, T., Qin, X. and Jin, Z., "Numerical study of the dehumidification structure optimization based on the modified model", *Energy Conversion and Management*, **181**, 159 (2019).

[22] Kuan, B. T. and Witt, P. J., "Modelling supersonic quenching of magnesium vapour in a Laval nozzle", *Chemical Engineering Science*, **87**, 23 (2013).

[23] Teixeira, A. M., Arinelli, L. O., Medeiros, J. and Araujo, O. Q. F., "Economic leverage affords post-combustion capture of 43 % of carbon emissions: Supersonic separators for methanol hydrate inhibitor recovery from raw natural gas and CO_2 drying", *Journal of Environmental Management*, **236**, 534 (2019).

[24] Wang, Y. and Hu, D., "Experimental and numerical investigation on the blade angle of axial flow swirling generator and drainage structure for supersonic separators with diversion cone", *Chemical Engineering Research and Design*, **133**, 155 (2018).

[25] Ma, Q. F., Hu, D. P., Jiang, J. Zh. and Qiu, Zh. H., "A turbulent Eulerian multi-fluid model for homogeneous nucleation

of water vapour in transonic flow", *International Journal of Computational Fluid Dynamics*, **23**, 221 (2009).

[26] Bian, J., Cao, X., Yang, W., Guo, D., Xiang, Ch., "Prediction of supersonic condensation process of methane gas considering real gas effects", *Applied Thermal Engineering*, **164**, 114508 (2020).

[27] Ding, H., Wang, Ch. and Chen, Ch., "Non-equilibrium condensation process of water vapor in moist air expansion through a sonic nozzle", *Flow Measurement and Instrumentation*, **40**, 238 (2014).

[28] Ding, H., Wang, Ch., Wang, G. and Chen, Ch., "Analytic equations for the Wilson point in high-pressure steam flow through a nozzle", *International Journal of Heat and Mass Transfer*, **91**, 961 (2015).

[29] Moses, C. A. and Stein, G. D., "On the growth of steam droplets formed in a Laval nozzle using both static pressure and light scattering measurements", *J. Fluids Eng.*, **100**, 311 (1977).

[30] Ishazaji, K., Ikohagi, T. and Daiuji, H., A high-resolution numerical method for transonic non-equiibrium condensation flows through a steam turbine cascade, *Proceedings of the 6th International Symposium on Computational Fluid Dynamics*, Lake Tahoe, CA, USA, 1, p. 484 (1995).

[31] Young, J. B., "Two-dimensional, nonequilibrium, wet-steam calculations for nozzles and turbine cascades", *Journal of Turbomachinery*, **114** (3), 569 (1992).